IEEE Access
Multidisciplinary | Rapid Review | Open Access Journal

Received July 14, 2020, accepted July 22, 2020, date of publication July 28, 2020, date of current version August 7, 2020.

Digital Object Identifier 10.1109/ACCESS.2020.3012535

Filter-Based Landweber Iterative Method for Reconstructing the Light Field

SHAN GAO AND GANGRONG QU
School of Science, Beijing Jiaotong University, Beijing 100044, China
Corresponding author: Gangrong Qu (grqu@bjtu.edu.cn)

This work was supported in part by the National Natural Science Foundation of China under Grant 61931003, and in part by the Fundamental Research Funds for the Central Universities under Grant 2019YJS197.

ABSTRACT The light field reconstruction aims to recover the 4D light field from the 3D focal stack, so it is a severe incomplete data reconstructing problem. The Landweber iteration is a general method to find the least-square solution of the discretized linear system, which is widely used for solving such problem. The relaxation strategies of the Landweber iteration are essential for both accelerating iterative convergence and decreasing errors. As a fast and non-approximate linear-time method, the fast guided filtering has good edge-preserving smoothing properties. It can be incorporated into the light field reconstruction process to improve the precision of the reconstructed results. In this paper, we propose a filter-based Landweber iterative method by introducing the optimized relaxation strategy and the fast guided filter. Specifically, the updated image in the iteration step contains the guidance image and the image obtained by the Landweber iteration, which makes the proposed method flexible. The experimental results show that the proposed method is more practical and effective compared with the relevant reconstruction methods.

INDEX TERMS Light field reconstruction, Landweber iteration, relaxation strategy, the fast guided filter.

I. INTRODUCTION

Computational imaging refers to digital image capture and processing techniques that combine computation and optical encoding. Light field imaging technology plays an important role in the development of computational imaging. Therefore, it is of great practical significance to collect or acquire light field data. The methods to acquire the light field are mainly divided into two categories: direct methods for 4D light field acquisition and indirect methods for light field reconstruction. Direct methods are to directly capture the light field by back-tracing the rays of the scene. The light field is represented by a set of 2D sub-aperture images captured from different viewpoints. The light field can be obtained by the plenoptic camera [1] and the camera array [2], which can improve or innovate the system structure of the original camera. Indirect methods reconstruct the light field by obtaining and calculating a part of the light field data, including coded mask data [3], [4] and focal stack data [5].

The associate editor coordinating the review of this manuscript and approving it for publication was Cesar Vargas-Rosales.

The focal stack can be captured by a fixed camera at different focuses. Ng Ren [6] revealed that the slices of the focal stack are 2D projections of the 4D light field. Therefore, if the focal stack is known, one can recover the light field by employing the reconstruction techniques used in computed tomography (CT). The inverse problem of recovering the light field can be regarded as the incomplete data reconstruction problem, which can be solved by the Landweber iterative method. Moreover, the fast guided filter is one of good edge-preserving smoothing methods. The filter yields both quality and efficiency in many applications, including noise reduction, detail smoothing, and joint upsampling. Therefore, we propose a Landweber iterative algorithm based on the fast guided filter. The sparse nature of the light field is used to store the entire projection matrix in memory. By minimizing the spectral radius of the matrix, an optimized strategy [7] is adopted to recover the light field.

The rest of the paper is organized as follows. In section II, the related work is introduced. In section III, we propose the discrete filter-based light field reconstruction method from the focal stack in which an optimized relaxation strategy is introduced. We show some experimental results in section IV.

Finally, our discussions and conclusions are presented in section V and VI separately.

II. RELATED WORK

Focal stack technology is an effective computational imaging method to reconstruct the light field. There are some reconstruction methods which introduce deconvolution in the spatial domain or inverse transform in frequency. Kubota *et al.* [8] proposed a linear filtering method to synthesize a dense light field using two sets of different images. The method is suitable for simple scenes with background and foreground objects, as well as it can realize dense light field synthesis and rendering. Kodama *et al.* [9] shifted pinholes on the lens based on 3D frequency to reconstruct all-in-focus images. Levin *et al.* [10] proposed a linear view synthesis method by averaging and deconvolving the spectra of all shifted focal stack images using a slope-invariant kernel. Mousnier *et al.* [11] applied a masked back-projection algorithm to partially reconstruct the light field by reconstructing epipolar images from the focal stack. Perez *et al.* [12] studied the inverse for the focal stack transform. A subset of the light field is obtained by this method.

Many researchers reconstructed the light field iteratively. Yin *et al.* [13] proposed a filter-based iterative method to reconstruct a 4D light field from the focal stack. The imaging equations are discretized into linear equations, and the filter-based iterative method was used to solve normal imaging equations. The projection matrix in [13] was not all stored in memory, so a certain row of projection matrix was generated when it was used. However, many analyses that need to transform the projection matrix (such as diagonalize a matrix or perform singular value decomposition on a matrix to find the generalized inverse of a matrix) are not applicable, which greatly restricts the research and development of iterative image reconstruction algorithms. Liu *et al.* [14] proposed the Landweber iterative scheme to obtain the high precision light field data and the scene depth of narrow viewing angles. The effect of the relaxation coefficient on the quality of the reconstructed light field remains to be further studied. Ito *et al.* [15] proposed the method of constructing the underlying dense light field from the sparse focal stack. The method can generate arbitrarily focused images. Lien *et al.* [16] reported a proof-of-concept light field scheme using transparent graphene photo-detector stacks. Based on a double stack of transport detectors, a linear iterative method for computational reconstruction of a 4D light field from a single exposure is proposed.

Thanks to the inherent similarity between CT image reconstruction and light field reconstruction, it is natural to solve light field reconstruction problems using the idea and technique from CT image reconstruction. Wu *et al.* proposed the image reconstruction method using image gradient $l_0 - norm$ and Tensor dictionary [17]. The method not only inherited the advantages of tensor dictionary learning but also preserved edge information. In the subsequent research, Wu *et al.* proposed the dictionary learning-based image-domain material composition methods for spectral CT [18] and the two-step regularization based method [19]. Xu *et al.* [20] proposed the l_0DL reconstruction technique by combining the dictionary learning and image gradient $l_0 - norm$. These methods can also be extended to the light field reconstruction.

The convergence behavior is of great importance, which often affects the quality of the reconstructed image. In [21], a general iterative scheme for image reconstruction was established in both simultaneous and block-iterative methods. As demonstrated in [21], the convergence of the general iterative scheme was explained under quite general conditions in both inconsistent and consistent case. As shown in [22], the convergence rate of the Landweber method was linear in the condition that the relaxation coefficient was a constant. [7] proposed the optimal relaxation method and established the relaxation strategy to accelerate the convergence when only the biggest singular value was known. These underlying theories are also applicable to iterative methods of light field reconstruction.

In this paper, we analyze the problem of the light field reconstruction from the focal stack by the filter-based iteration method. Recovering the light field from the focal stack can be regarded as an ill-posed problem, and Landweber iterative methods in CT are suitable for solving such kind of problem. Motivated by the idea in [7], the optimal relaxation strategy based on the sparseness of the light field is introduced to the proposed method.

III. THE METHOD TO RECONSTRUCT THE LIGHT FIELD

A. IMAGING MODEL

Classical radiometry shows that the irradiance from the aperture of a lens onto a point (x, y) on the film is equal to the following weighted integral of the radiance coming through the lens [6].

$$E_F^c(x,y) = \frac{1}{F^2}\int\int \overline{L}_F^c\left(x^c, y^c, u^c, v^c\right)\cos^4\theta\, du dv, \quad (1)$$

where F is the separation between the exit pupil of the lens and the film, $E_F^c(x,y)$ is the irradiance on the film at position (x,y), $\overline{L}_F^c$ is the light field, $\cos^4\theta$ is a falloff factor referred to as optical vignetting. We define $\overline{L}_F^c(x,y,u,v)\cos^4\theta = L_F^c(x,y,u,v)$. Equation (1) can be further simplified by ignoring the constant term $\frac{1}{F^2}$,

$$E_F^c(x,y) = \int\int L_F^c(x,y,u,v)\, du dv. \quad (2)$$

Its discrete form is

$$E_F(x,y) = \sum_u \sum_v L_F(x,y,u,v), \quad (3)$$

where, L_F is the discrete light field, E_F is the image. If we consider the light field focused on F_m,

$$L_{F_m}(x,y,u,v) = L_F\left(\left(1-\frac{1}{\alpha_m}\right)u + \frac{x}{\alpha_m}, \left(1-\frac{1}{\alpha_m}\right)v + \frac{y}{\alpha_m}, u, v\right), \quad (4)$$

where $\alpha_m = \frac{F_m}{F}$. The irradiance of the recorded image at pixels (x, y) with the depth F_m is,

$$\begin{aligned} &E_{F_m}(x,y) \\ &= \overline{E}_{F_m}(\alpha_m x, \alpha_m y) \\ &= \sum_{u_i}\sum_{v_i} L_F^{(u_i,v_i)}((\alpha_m-1)u_i + x, (\alpha_m-1)v_i + y) \\ &= \sum_i L_F^i((\alpha_m-1)u_i + x, (\alpha_m-1)v_i + y), \end{aligned} \tag{5}$$

where $L_F^{(u_i,v_i)} = L_F^i$ denotes the sub-aperture image from a certain viewpoint, with the index i of it. E_{F_m} is the FOV corrected image difference. In this paper, it is assumed all the images have been FOV corrected with the image registration technique [23]–[25]. Rewrite (5) into matrix form,

$$A_m \begin{bmatrix} L_F^1 \\ \vdots \\ L_F^N \end{bmatrix} = E_{F_m}, \tag{6}$$

where, A_m is the projection matrix, L_F^i is the sample of the light field. Suppose there are M slices of focal stack, the linear system can be expressed as

$$AX = b, \tag{7}$$

where, $A = [A_1, \ldots, A_M]^T$, $X = [L_F^1, \ldots, L_F^N]^T$, and $b = [E_{F_1}, \ldots, E_{F_M}]^T$. Matrix A projects sub-aperture images (the light field) onto a series of images focused at different positions. The matrix A can be stored sparsely, which greatly reduced the storage space.

B. FAST GUIDED FILTER

The guided filter [26] shares the nice property of edge-preserving smoothing and it can be computed more effectively and properly compared with the bilateral filter [27]–[30]. Derived from a local linear model, the filter can be computed in $O(N)$ time. And the fast guided filter [31] speeds up from $O(N)$ time to $O(N/s^2)$ time.

Assuming that the guidance is I, and the filtering output is q. In a window centered at the pixel k, q is a linear transform of I:

$$q_i = a_k I_i + b_k, \quad \forall i \in \omega_k, \tag{8}$$

where (a_k, b_k) are linear coefficients assumed to be constants in ω_k with a square window of a radius r. The solution of (8) can be obtained by minimizing the cost function,

$$E(a_k, b_k) = \sum_{i\in\omega_k}((a_k I_i + b_k - p_i)^2 + \epsilon a_k^2). \tag{9}$$

The regularization parameter ϵ is a constant. To solve (9), we get

$$a_k = \frac{\frac{1}{|\omega|}\sum_{i\in\omega_k} I_i p_i - \mu_k \overline{p}_k}{\sigma_k^2 + \epsilon}, \tag{10}$$

$$b_k = \overline{p}_k - a_k \mu_k, \tag{11}$$

where μ_k and σ_k^2 denote the mean and variance in window ω_k, $|\omega|$ is the number of pixels in ω_k, $\overline{p}_k = \frac{1}{|\omega|}\sum_{i\in\omega_k} p_i$ is the mean of p in the window.

For a given pixel i, it changes with different overlapping window ω_k. So we average the possible values of q_i. Equation (8) can be rewritten as

$$q_i = \frac{1}{|\omega|}\sum_{k|i\in\omega_i}(a_k I_i + b_k) = \overline{a}_i I_i + \overline{b}_i. \tag{12}$$

Here, $\overline{a}_i = \frac{1}{|\omega|}\sum_{i\in\omega_i} a_k$, $\overline{b}_i = \frac{1}{|\omega|}\sum_{i\in\omega_i} b_k$. We can get the fast guided filter by subsampling the p and the guidance I for a ratio s.

C. THE FILTER-BASED ITERATIVE METHOD

There are several classic Landweber iteration methods, such as algebraic reconstruction technique (ART) [32], simultaneous iterative reconstruction technique (SIRT) [33], and simultaneous algebraic reconstruction technique (SART) [34]. SART algorithm maintains the convergence speed of ART method, and also takes into account the noise suppression ability of SIRT method. In this paper, SART iterative scheme is adopted for the iterative solution. Based on the fast guided filter, the method can further improve the quality of the results.

Based on the linear system,

$$AX = b. \tag{13}$$

Assuming that there are M slices of the focal stack with dimension $P \times Q$ of each slice. Then the dimension of projection matrix A is $I \times J = (P \times Q \times M) \times (P \times Q \times N)$, the dimension of X is $(P \times Q \times N) \times 1$, and the dimension of b is $(P \times Q \times M) \times 1$.

A can be obtained based on (5) using the bilinear interpolation algorithm. The value of the E_{F_m} at the pixel (x, y) is equivalent to the integral of L_F^i for all different viewpoints. The pixel $((\alpha_m-1)u_i+x, (\alpha_m-1)v_i+y)$ might be a fraction, then we estimate this value by the bilinear interpolation algorithm. Assume $(\alpha_m - 1)u_i + x = m_0 + a$, $(\alpha_m - 1)v_i + y = n_0 + b$, where m_0, n_0 are integers, $0 < a < 1, 0 < b < 1$. Then,

$$\begin{aligned} &L_F^i((\alpha_m-1)u_i + x, (\alpha_m-1)v_i + y) \\ &= (1-a)(1-b)L_F^i(m_0, n_0) + a(1-b)L_F^i(m_0+1, n_0) \\ &\quad +(1-a)bL_F^i(m_0, n_0+1) + abL_F^i(m_0+1, n_0+1). \end{aligned} \tag{14}$$

According to (14), there are at most $4 \times N$ elements for each row of matrix A, so A is sparse.

The Landweber iterative scheme is

$$X^{(n+1)} = X^{(n)} + \lambda_n V^{-1} A^T W\left(b - AX^{(n)}\right), \tag{15}$$

where, $W = \frac{1}{A_{i,+}}$, $V = A_{+,j}$, $A_{i,+} = \sum_{j=1}^{J}\left|A_{i,j}\right|$, $(i = 1, \ldots I)$, $A_{+,j} = \sum_{i=1}^{I}\left|A_{i,j}\right|$, $(j = 1, \ldots J)$.

Since M slices of focal stack need to be performed in each iteration, we can further divide the iteration step into sub-iteration. Suppose the initial value of each iteration $(n+1)$ is $X^{(n+1,0)}$. The formula of sub-iteration is

$$X^{(n+1,m)} = X^{(n+1,m-1)} + \lambda_{n+1} V^{-1} A^T W \left(b - AX^{(n+1,m-1)}\right). \quad (16)$$

The steps of the iteration method based on the fast guided filter are as follows:

(1) initialize variables with the sub-aperture image $X^{(n,m)} = 0, n = 1, m = 1$, the number of iteration rounds N, the regularization parameter ϵ, a ratio s, and the window radius r;

(2) calculate the correction matrix by $Corr^{(n,m-1)} = V^{-1}A^T W \left(b - AX^{(n,m-1)}\right)$;

(3) calculate the matrix $X^{(n,m)}$ of the round m by $X^{(n,m)} = X^{(n,m-1)} + \lambda_n V^{-1} A^T W \left(b - AX^{(n,m-1)}\right)$;

(4) repeat the process from (2) to (3) until the sub-iteration reaches M times;

(5) weight the value obtained by (4) and its filtered value, and regard this weight value as the initial value of the next iteration,

$$\begin{aligned} X^{(n+1,0)} &= \alpha X_{guided} + \beta X^{(n,M)} \\ &= (\alpha \overline{a} + \beta) X^{(n,M)} + \overline{b} \\ &= \overline{X}^{(n,M)}, \end{aligned} \quad (17)$$

where α and β are the coefficients, and $\alpha + \beta = 1$. The computation of X_{guided} follows (12). Repeat steps (2) - (5) until the convergence requirement or the specified number of iterations are reached.

In Landweber iteration, the value of the relaxation coefficient λ_n is important, which directly affects the accuracy of the iterative solution. We can easily expand the Landweber iteration strategy proposed by [7] into our method.

Based on Landweber method, the weighted Landweber iteration scheme (15) can be transformed into the Landweber iteration scheme without weight. If we let $Z^{(n)} = V^{\frac{1}{2}} X^{(n)}, G = W^{\frac{1}{2}} A V^{-\frac{1}{2}}, \overline{b} = W^{\frac{1}{2}} b$, then we have

$$Z^{(n+1)} = Z^{(n)} + \lambda_n G^T \left(\overline{b} - GZ^{(n)}\right). \quad (18)$$

Let $\{\mu_k\}_{k=1}^m$ be the distinct positive eigenvalues of $G^T G$ that are ordered such that $\mu_1 > \cdots > \mu_m > 0$. The spectral norm or the 2-norm of the matrix G is

$$\|G\|^2 = \mu_1. \quad (19)$$

For a large matrix G, the computation of the smaller positive eigenvalue μ_m is time consuming. Because $\mu_1 = \|G\|_2^2$, we can get the biggest eigenvalue by calculating $\|G\|_2^2$. Due to μ_m is unknown, one strategy of the coefficient is that

$$\lambda_n = \frac{2}{\omega \mu_1}, \quad \omega \in (1, 2), \quad n = 1, 2, \ldots \quad (20)$$

For the filter-based iteration method we put forward, Algorithm 1 shows the algorithm flow of the iteration process.

Algorithm 1 Iteration Algorithm

Input:

A sequence of M focal stack I_{pq}, the corresponding factor α, β, number of iteration rounds N, the window radius r, the regularization parameter ϵ, a ration s, and the original light field L_{F0}.

Output:

The projection matrix A;
The light field L_F;
BRISQUE *bri* or SSIM *ssim*, PSNR *psnr*.

for $m = 1$ to M **do**
  for $p = 1$ to P **do**
    for $q = 1$ to Q **do**
      Calculate the projection matrix A by (5) using bilinear interpolation algorithm.
    end for
  end for
end for
Solve the biggest eigenvalue μ_1 of $G^T G$, then relaxation coefficient is $\lambda_n = \frac{2}{\omega \mu_1}$, $\omega \in (1, 2)$.
for $n = 1$ to N **do**
  for $m = 1$ to M **do**
    Calculate the light field L_F by (15).
  end for
end for
for $n = 1$ to N **do**
  Obtain the index BRISQUE *bri*.
  Or obtain the index SSIM *ssim* and PSNR *psnr*.
end for

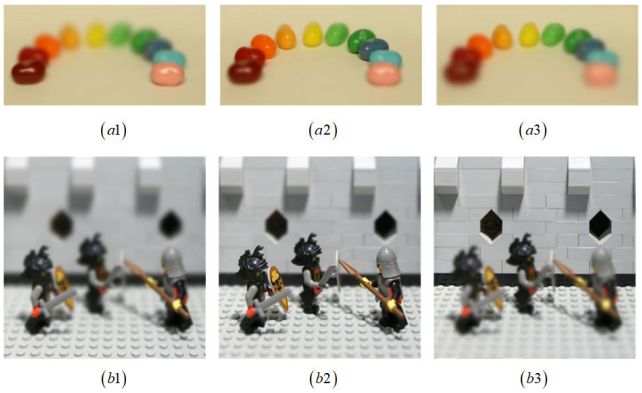

FIGURE 1. The focal stack of JellyBeans and LegoKnights on the front plane, the middle plane and the back plane.

IV. EXPERIMENTS AND RESULTS

In this section, we present experimental evaluations and discussions about our proposed method. We take three types of focal stack data:

(1) the focal stack data synthesized from the Stanford light field archive [35], which is sampled with 17×17 angular resolution;

(2) the data which is captured with a Lytro light field camera [11];

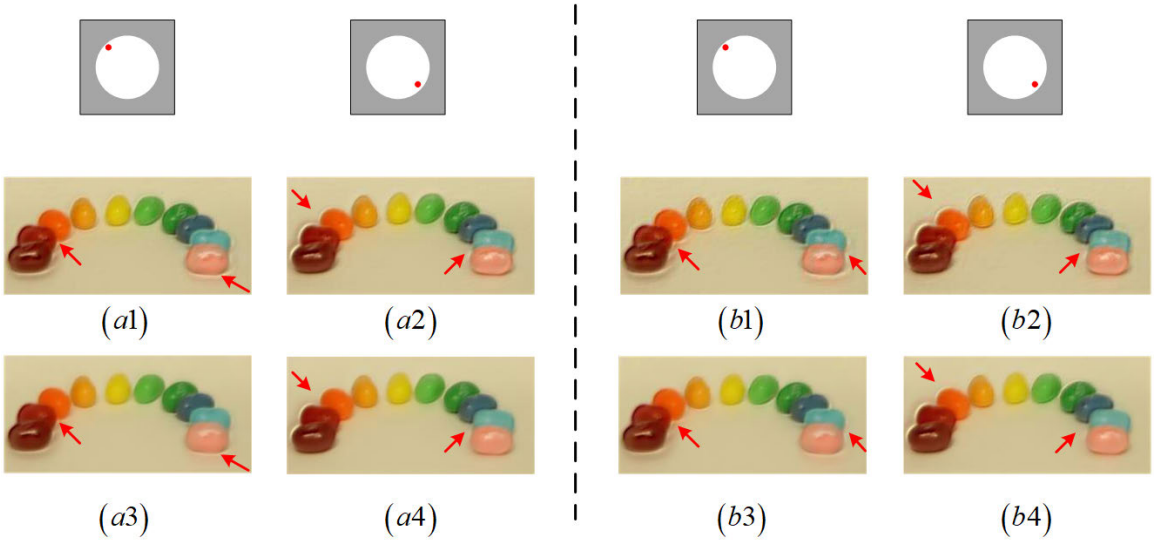

FIGURE 2. The light field(JellyBeans) reconstructed by SART method and the proposed method. (a1) (a2) (b1) and (b2) are results of the SART method. (a3) (a4) (b3) and (b4) are results of the proposed method. The relaxation coefficient measured by the left of the dotted line is 0.5 and the right is 1.5.

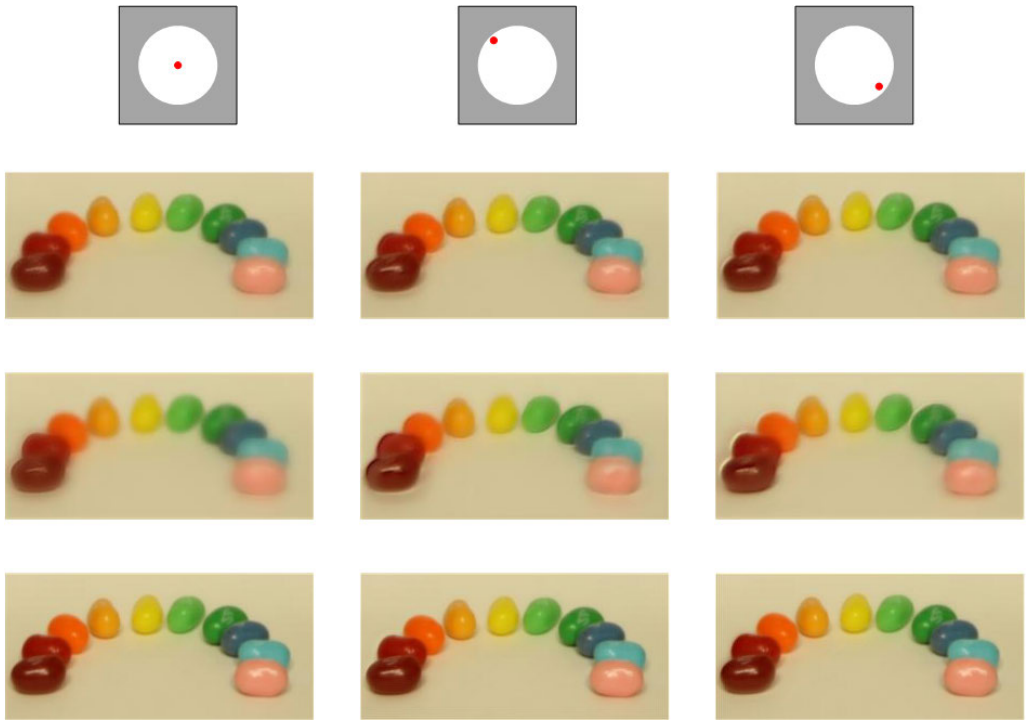

FIGURE 3. The reconstructed light field from a sequence of 14 images on JellyBeans of relaxation strategy $\lambda = 0.172$ and methods in [10], [13]. We have included a supplementary avi file which contains the reconstructed light field of JellyBeans experiments with $\lambda = 0.172$. This will be available at `http://ieeexplore.ieee.org`.

(3) and the real data which is captured by the Basler camera (Model:acA411220uc) and the Myutron prime lens (Model:HF5018V) with an F-number of $f/1.6$ and the focal length of $f = 25mm$.

In order to illustrate the performance of the proposed algorithms, we compare our method with SART method and methods in [10], [13]. The experiments are carried out by MATLAB codes on Intel(R) Core(TM) i5-7200U CPU 2.50 GHz with 8 GB RAM.

To test the feasibility and accuracy of the method, we compute the structural similarity index metric(SSIM) [36], peak signal to noise ratio(PSNR) and dubbed blind/referenceless image spatial quality evaluator(BRISQUE) [37], [38] of the reconstructed image. SSIM is used to analyze the quality

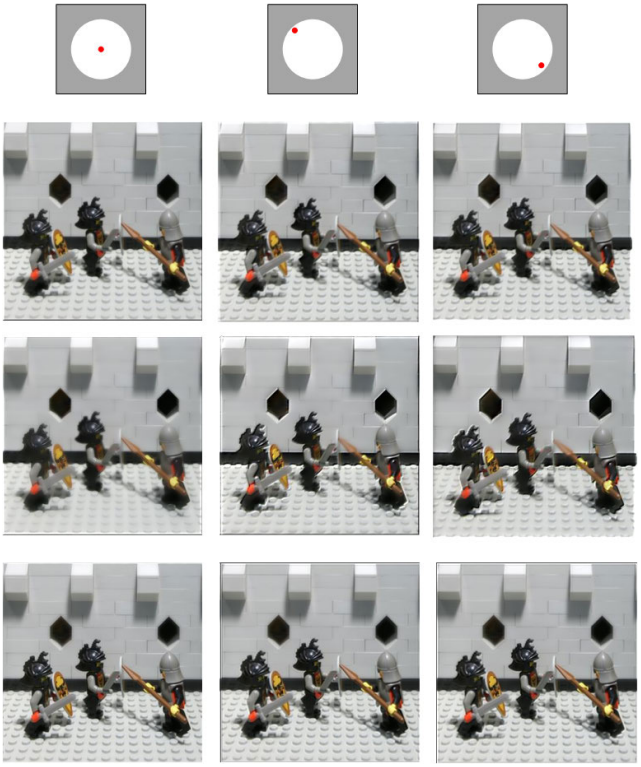

FIGURE 4. The reconstructed light field from a sequence of 21 images on LegoKnights of relaxation strategy $\lambda = 0.1$ and methods in [10], [13]. We have included a supplementary avi file which contains the reconstructed light field of LegoKnights experiments with $\lambda = 0.1$. This will be available at `http://ieeexplore.ieee.org`.

TABLE 1. The SSIM and PSNR of the light field(JellyBeans) after three rounds.

	$\lambda_n = 0.5$		$\lambda_n = 0.5$	
index	SSIM	PSNR	SSIM	PSNR
our method	**0.9035**	**16.6478**	**0.8948**	**15.4332**
SART method	0.8964	16.0458	0.8918	15.0516

of the reconstructed light field and measures the similarity between two images, which characterizes image similarity in terms of brightness, contrast and structure. The larger the value is, the better the result is. PSNR is the ratio between the maximum possible power of a signal and the power of corrupting noise that affects the fidelity of its representation. The larger PSNR indicates the better result. BRISQUE is a natural scene statistic-based distortion-generic blind/no-reference (NR) image quality assessment (IQA) model that operates in the spatial domain. The reconstructed result is better with the smaller value.

A. IN COMPARISON WITH SART METHOD

To verify the effect of the fast guided filter, we compare our method with SART method in the condition of the same relaxation coefficient. The first row of Fig. 1 is the focal stack of JellyBeans. Fig. 2 is the reconstruction result of our method and SART method. Table. 1 is the quantitative evaluation result. From Fig. 2, the proposed method with the fast guided

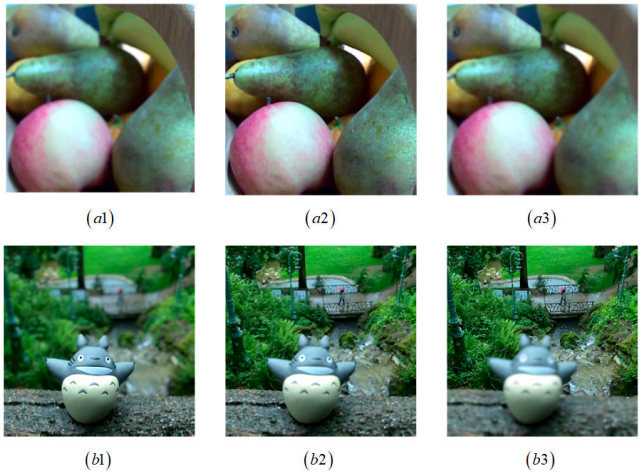

FIGURE 5. The focal stack of fruits and totoro on the front plane, the middle plane and the back plane.

filter can preserve edges and reduce the noise of the image in comparison with SART method. From Table. 1, it can be observed that our proposed method achieves higher PSNR and SSIM.

B. EXPERIMENTAL RESULTS WITH THREE TYPES OF DATA

1) EXPERIMENTS WITH LIGHT FIELD ARCHIVE

For the first type of experiment, we use two light field data, JellyBeans and LegoKnights. We synthesize the focal stack with 14 slices for Jelly Beans and 21 slices for LegoKnights based on MATLAB light field toolbox [39], [40], as shown in Fig. 2. And we evaluate our method based on SSIM and PSNR.

For the JellyBeans experiment, we can get the biggest eigenvalue of $G^T G$ is $\mu_1 = 5.8184$. The parameter ϵ for the fast guided image filtering is set to 0.0001, the filter window radius is $r = 3$, the ratio is 3 and parameters $\alpha = 0.8947$, $\beta = 0.1053$ for the JellyBeans experiments. We use three schemes to reconstruct the light field.

(1) $\lambda_n = 0.172, n = 1, 2$;
(2) $\lambda_n = 1, n = 1, 2$ based on [13];
(3) Levin's(linear view synthesis) method based on [10].

For the LegoKnights experiment, we can get the biggest eigenvalue of $G^T G$ is $\mu_1 = 10.689$. The filter is set to $\epsilon = 0.0001$, the window radius is $r = 3$, the ratio is 1, and $\alpha = 0.1667$, $\beta = 0.8333$. We use three schemes to reconstruct the light field.

(1) $\lambda_n = 0.1, n = 1, 2, 3$;
(2) $\lambda_n = 1, n = 1, 2, 3$ based on [13];
(3) Levin's(linear view synthesis) method based on [10].

The reconstructed results of different methods are shown in Fig. 3 and Fig. 4. The SSIM and PSNR to evaluate the image clarity are shown in Table 2. According to [7], the range of the optimal relaxation coefficient is $\lambda_n \in (0.1719, 0.3437)$ for JellyBeans and $\lambda_n \in (0.0936, 0.1871)$ for LegoKnights. And our methods with the strategy

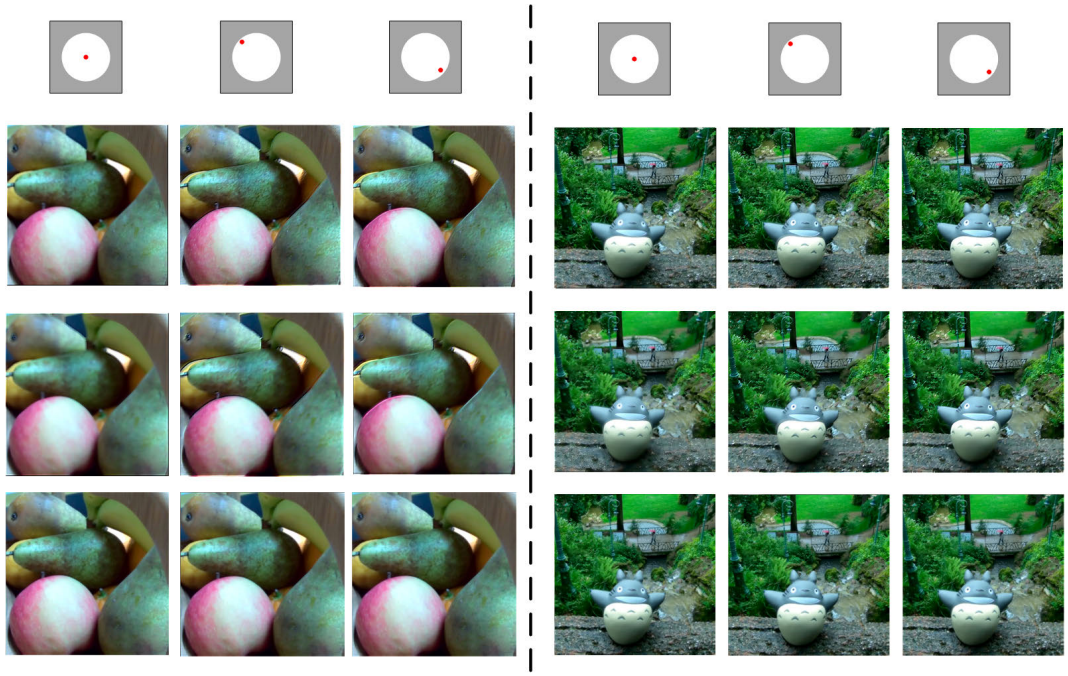

FIGURE 6. The reconstructed light field from a sequence of 12 images on fruits(from top to bottom on the left: $\lambda_n = 0.43$, $\lambda_n = 1$ in [13], Levin's method [10]) and from a sequence of 14 images on totoro(from top to bottom on the right: $\lambda_n = 0.25$, $\lambda_n = 1$ in [13], Levin's method [10]). We have included supplementary avi files which contain the reconstructed light field of fruits experiments with $\lambda = 0.43$ and totoro experiments with $\lambda = 0.25$. This will be available at http://ieeexplore.ieee.org.

TABLE 2. Light field clarity comparison from the stanford light field archive.

JellyBeans			LegoKnights		
λ_n	SSIM	PSNR	λ_n	SSIM	PSNR
0.172	**0.9251**	**17.8319**	0.1	**0.7275**	**18.3135**
1 [13]	0.9008	16.0307	1 [13]	0.6852	15.4811
Levin's method [10]	0.8803	17.8090	Levin's method [10]	0.6344	17.3100

$\lambda_n = 0.172$ for JellyBeans and the strategy $\lambda_n = 0.1$ for LegoKnights perform better than methods in [10], [13].

2) EXPERIMENTS WITH LYTRO CAMERA

Due to the lack of ground truth data, we calculate BRIQUE to verify the reconstructed results in the Lytro experiments. For the fruits experiment, the parameter ϵ for the fast guided image filtering is set to 0.0001, the filter window radius is $r = 3$, a ratio is 3 and parameters $\alpha = 0.1$, $\beta = 0.9$. We can get the biggest eigenvalue of $G^T G$ is $\mu_1 = 4.6176$ in fruits experiments. We use three schemes to reconstruct the light field.

(1) $\lambda_n = 0.43, n = 1, 2 \ldots, 4$;
(2) $\lambda_n = 1, n = 1, 2 \ldots, 4$ based on [13];
(3) Levin's(linear view synthesis) method based on [10].

For the totoro experiment, we can get the biggest eigenvalue of $G^T G$ is $\mu_1 = 4.0535$. The parameter ϵ for the fast guided image filtering is set to 0.0001, the filter window radius is $r = 3$, a ratio is 1 and parameters $\alpha = 0.1053$, $\beta = 0.8947$. We use three schemes to reconstruct the light field.

(1) $\lambda_n = 0.25, n = 1, 2$;
(2) $\lambda_n = 1, n = 1, 2$ based on [13];
(3) Levin's(linear view synthesis) method based on [10].

Fig. 5 shows the focal stack of fruits and totoro experiments. Fig. 6 is the reconstructed result of fruits experiment and totoro experiment. According to [7], the range of the optimal relaxation coefficient is $\lambda_n \in (0.2166, 0.4331)$ for fruits. From Fig. 7(a), we find that our method with the strategy $\lambda_n = 0.43$ performs better than other methods when the iteration reaches 4. The range of the optimal relaxation coefficient is $\lambda_n \in (0.2467, 0.4934)$ for totoro according to [7]. From Fig. 7(b), we find that our method with the strategy $\lambda_n = 0.25$ achieves optical convergence results when the number of iteration reaches 2. And our method's convergence speed is faster than the method in [13]. The growth of BRIQUE after some iterations can be attributed to the noise and quantization error. From Fig. 8, we can find that the result in (b) has unnecessary artifacts, results in (c) and (d) lost image details. The result in (a) performs better than others.

3) EXPERIMENTS WITH REAL DATA

The captured focal stack data consists of 16 images. For the real experiment, the parameter ϵ for the fast guided image filtering is set to 0.0001, the filter window radius is $r = 3$, a ratio is 3 and parameters $\alpha = 0.3$, $\beta = 0.7$. We can get the biggest eigenvalue of $G^T G$ is $\mu_1 = 7.114$ in the experiments. We use three schemes to reconstruct the light field.

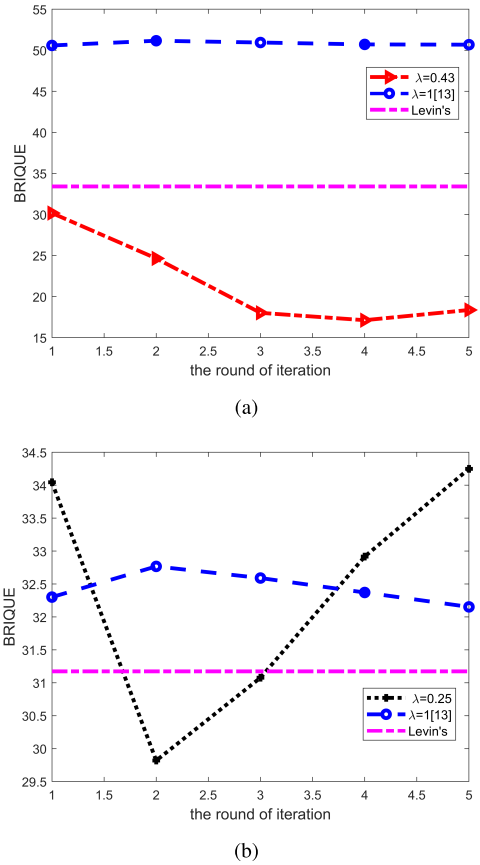

FIGURE 7. Convergence analysis curve. (a) The convergence curve of fruits experiments. (b) The convergence curve of the totoro experiments.

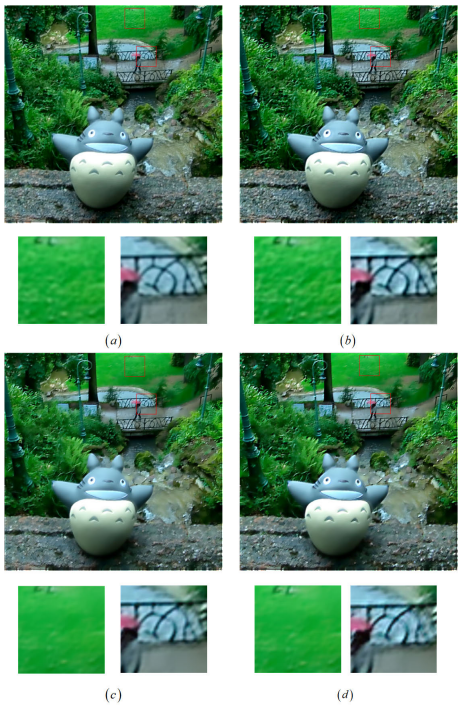

FIGURE 8. The reconstructed light field of totoro experiment from the upper left view. (a) The reconstructed light field of our method after 2 iterations; (b) The reconstructed light field of our method after 5 iterations; (c) The reconstructed light field of method in [13] after 2 iterations; (d) The reconstructed light field of method in [13] after 5 iterations.

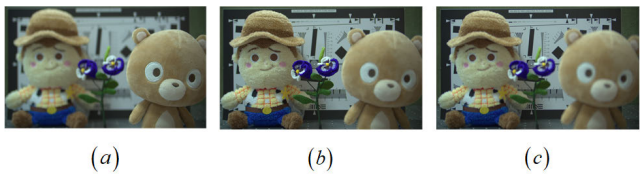

FIGURE 9. The focal stack of pets on the front plane, the middle plane and the back plane.

(1) $\lambda_n = 0.15, n = 1, 2, 3$;
(2) $\lambda_n = 1, n = 1, 2, 3$ based on [13];
(3) Levin's(linear view synthesis) method based on [10].

Fig. 9 shows the focal stack of pets experiments. Fig. 10 is reconstructed results of pets experiment. From Fig. 11, we find that our method performs better than other methods in [10], [13]. From the close-up views of local details, we can find our method shows higher accuracy and better behavior.

V. DISCUSSIONS

In this paper, there are several coefficients for us to adjust, λ_n, α, and β. The relaxation strategy λ_n is determined when the biggest singular value of the projection matrix is available. The trade-off of α and β is empirically determined in our method. Parameter adjustment of α and β remains as one of the issues to further study to improve the quality of the results. The interpolation methods also have an influence on the accuracy of the reconstructed results. We adopt the bilinear interpolation algorithm to obtain the projection matrix. There are lots of other interpolation methods that can be studied, such as Newton mean square interpolation and spline interpolation. In addition, it only takes a few minutes to run our program and the computation time is shown in Table 3.

TABLE 3. Computation time of reconstructing the light field.

data	size	slices	iterations	time(s)
JellyBeans	$150 \times 300 \times 3$	14	2	84
LegoKnights	$300 \times 300 \times 3$	21	3	261
fruits	$544 \times 544 \times 3$	12	4	524
totoro	$544 \times 544 \times 3$	14	2	436
pets	$594 \times 981 \times 3$	16	3	1128

Compared with [13], our method has more feasibility. The updated image in our method contains the information in the guidance image and in the image reconstructed by SART algorithm. Reference [13] directly adopted the guided filter to the prior image in each sub-iteration and the coefficient of [13] defaulted to 1.

The Levin's method [10] computed a shifted average of the focal stack and obtained the perspective shift by deconvolving the average image. The slope range of the focal stack is much larger than that of the actual objects. While, in our

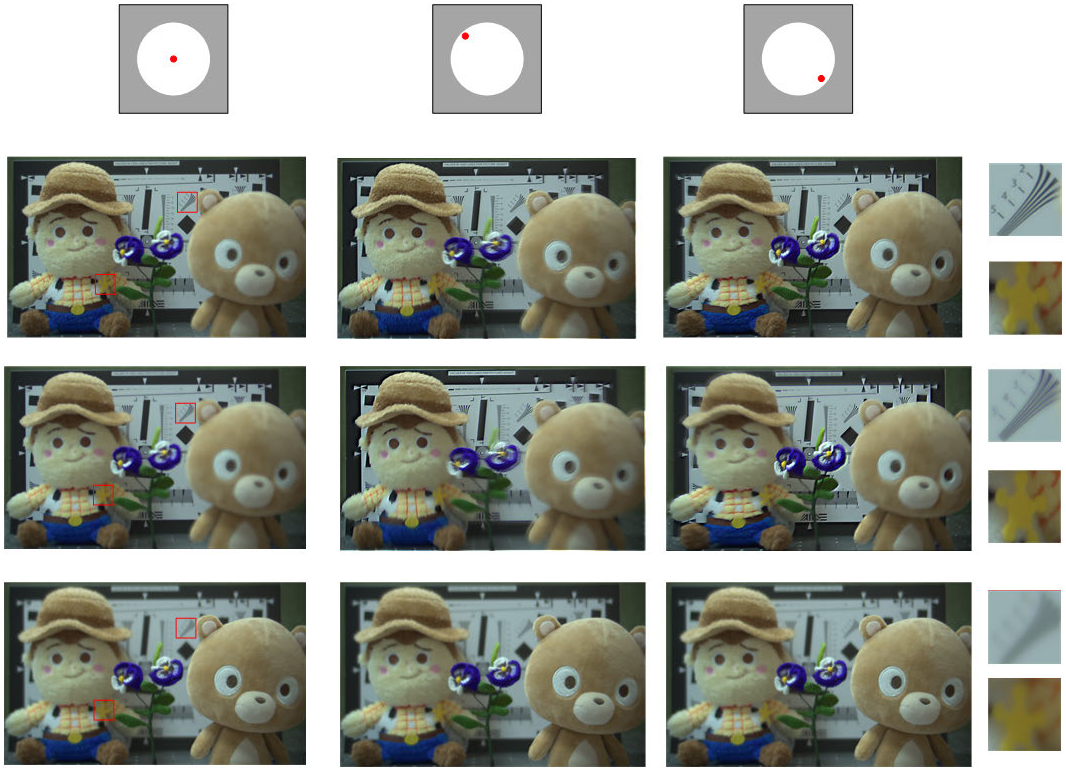

FIGURE 10. The reconstructed light field from a sequence of 16 images on pets of relaxation strategy $\lambda = 0.15$ and methods in [10], [13]. We have included a supplementary avi file which contains the reconstructed light field of real experiments with $\lambda = 0.15$. This will be available at `http://ieeexplore.ieee.org`.

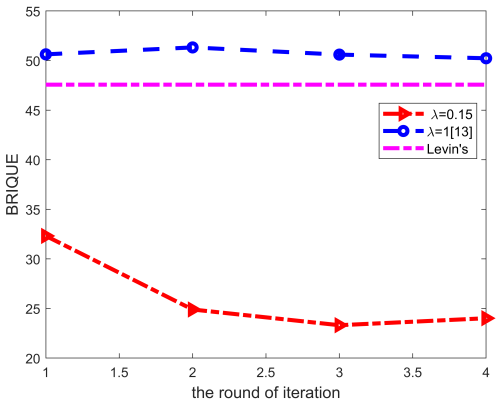

FIGURE 11. The reconstructed light field of the real data for different strategies.

experiments, the slope range of the focal stack is almost the same with the actual objects' range. The proposed method is experimentally observed to be more robust to variations in image capturing conditions, such as the number of images and the depth ranges of the focal stack.

VI. CONCLUSION

In this study, we proposed the filter-based Landweber iterative method to reconstruct the light field. Firstly, the focal stack imaging process was discretized into linear equations, in which the projection matrix was stored as a sparse mode. Then, we reconstructed the light field iteratively, in which we merged the guidance image. Furthermore, the relaxation strategy was also considered to improve the precision of the reconstructed light field. In comparison with state-of-art methods, the experiments showed that the light field reconstructed by our method performed better in reconstruction accuracy and visual effects.

Since acquiring the focal stack corresponds to obtaining the projection in CT, the light field reconstruction from the focal stack corresponds to the image reconstruction from projections. Therefore, the methods and technologies in CT are of referential and enlightening implications for the theories and applications of the light field imaging. How to apply the newly developed CT algorithm to the light field reconstruction is worth studying. We can further study the image prior and the regularizer in CT reconstruction to optimize our iterative method. Once we get a high-precision light field, we can realize many computer vision and graphics applications, involving 3D scene reconstruction and depth reconstruction.

REFERENCES

[1] R. Ng, M. Levoy, M. Brédif, G. Duval, M. Horowitz, and P. Hanrahan, "Light field photography with a hand-held plenoptic camera," *Comput. Sci. Tech. Rep.*, vol. 2, no. 11, pp. 1–11, 2005.

[2] B. Wilburn, N. Joshi, V. Vaish, E.-V. Talvala, E. Antunez, A. Barth, A. Adams, M. Horowitz, and M. Levoy, "High performance imaging using large camera arrays," *ACM Trans. Graph.*, vol. 24, no. 3, pp. 765–776, Jul. 2005.

[3] A. Veeraraghavan, R. Raskar, A. Agrawal, A. Mohan, and J. Tumblin, "Dappled photography: Mask enhanced cameras for heterodyned light fields and coded aperture refocusing," *ACM Trans. Graph.*, vol. 26, no. 3, p. 69, 2007.
[4] C. K. Liang, T. H. Lin, B. Y. Wong, C. Liu, and H. H. Chen, "Programmable aperture photography: Multiplexed light field acquisition," *ACM Trans. Graph.*, vol. 27, no. 3, p. 55, 2008.
[5] K. Takahashi, Y. Kobayashi, and T. Fujii, "From focal stack to tensor light-field display," *IEEE Trans. Image Process.*, vol. 27, no. 9, pp. 4571–4584, Sep. 2018.
[6] R. Ng and P. M. Hanrahan, *Digital Light Field Photography*. Stanford, CA, USA: Stanford Univ. Press, 2006.
[7] G. Han, G. Qu, and M. Jiang, "Relaxation strategy for the landweber method," *Signal Process.*, vol. 125, pp. 87–96, Aug. 2016.
[8] A. Kubota, K. Aizawa, and T. Chen, "Reconstructing dense light field from array of multifocus images for novel view synthesis," *IEEE Trans. Image Process.*, vol. 16, no. 1, pp. 269–279, Jan. 2007.
[9] K. Kodama and A. Kubota, "Efficient reconstruction of all-in-focus images through shifted pinholes from multi-focus images for dense light field synthesis and rendering," *IEEE Trans. Image Process.*, vol. 22, no. 11, pp. 4407–4421, Nov. 2013.
[10] A. Levin and F. Durand, "Linear view synthesis using a dimensionality gap light field prior," in *Proc. IEEE Comput. Soc. Conf. Comput. Vis. Pattern Recognit.*, Jun. 2010, pp. 1831–1838.
[11] A. Mousnier, E. Vural, and C. Guillemot, "Partial light field tomographic reconstruction from a fixed-camera focal stack," 2015, *arXiv:1503.01903*. [Online]. Available: http://arxiv.org/abs/1503.01903
[12] F. Pérez, A. Pérez, M. Rodríguez, and E. Magdaleno, "Lightfield recovery from its focal stack," *J. Math. Imag. Vis.*, vol. 56, no. 3, pp. 573–590, Nov. 2016.
[13] X. Yin, G. Wang, W. Li, and Q. Liao, "Iteratively reconstructing 4D light fields from focal stacks," *Appl. Opt.*, vol. 55, no. 30, pp. 8457–8463, 2016.
[14] C. Liu, J. Qiu, and M. Jiang, "Light field reconstruction from focal stack based on landweber iterative scheme," in *Proc. Math. Imag.*, 2017, p. MM2C-3.
[15] D. Ito, K. Takahashi, and T. Fujii, "Generating arbitrarily focused images from sparse focal stack through light field reconstruction," in *Proc. Int. Workshop Adv. Image Technol. (IWAIT)*vol. 11049, Mar. 2019, Art. no. 110493E.
[16] M.-B. Lien, C.-H. Liu, I. Y. Chun, S. Ravishankar, H. Nien, M. Zhou, J. A. Fessler, Z. Zhong, and T. B. Norris, "Ranging and light field imaging with transparent photodetectors," *Nature Photon.*, vol. 14, no. 3, pp. 143–148, Mar. 2020.
[17] W. Wu, Y. Zhang, Q. Wang, F. Liu, P. Chen, and H. Yu, "Low-dose spectral CT reconstruction using image gradient ℓ_0–norm and tensor dictionary," *Appl. Math. Model.*, vol. 63, pp. 538–557, Nov. 2018.
[18] W. Wu, H. Yu, P. Chen, F. Luo, F. Liu, Q. Wang, Y. Zhu, Y. Zhang, J. Feng, and H. Yu, "DLIMD: Dictionary learning based image-domain material decomposition for spectral CT," 2019, *arXiv:1905.02567*. [Online]. Available: http://arxiv.org/abs/1905.02567
[19] W. Wu, P. Chen, V. V. Vardhanabhuti, W. Wu, and H. Yu, "Improved material decomposition with a two-step regularization for spectral CT," *IEEE Access*, vol. 7, pp. 158770–158781, 2019.
[20] M. Xu, D. Hu, F. Luo, F. Liu, S. Wang, and W. Wu, "Limited angle X ray CT reconstruction using image gradient ℓ_0 norm with dictionary learning," *IEEE Trans. Radiat. Plasma Med. Sci.*, early access, May 6, 2020, doi: 10.1109/TRPMS.2020.2991887.
[21] M. Jiang and G. Wang, "Convergence studies on iterative algorithms for image reconstruction," *IEEE Trans. Med. Imag.*, vol. 22, no. 5, pp. 569–579, May 2003.
[22] J. Wang and Y. Zheng, "On the convergence of generalized simultaneous iterative reconstruction algorithms," *IEEE Trans. Image Process.*, vol. 16, no. 1, pp. 1–6, Jan. 2007.
[23] P. Thevenaz, U. E. Ruttimann, and M. Unser, "A pyramid approach to subpixel registration based on intensity," *IEEE Trans. Image Process.*, vol. 7, no. 1, pp. 27–41, Jan. 1998.
[24] B. He, G. Wang, X. Lin, C. Shi, and C. Liu, "High-accuracy sub-pixel registration for noisy images based on phase correlation," *IEICE Trans. Inf. Syst.*, vol. E94-D, no. 12, pp. 2541–2544, 2011.
[25] Q. Miao, G. Wang, and X. Lin, "Kernel based image registration incorporating with both feature and intensity matching," *IEICE Trans. Inf. Syst.*, vol. E93-D, no. 5, pp. 1317–1320, 2010.
[26] K. He, J. Sun, and X. Tang, "Guided image filtering," in *Proc. Eur. Conf. Comput. Vis.* Berlin, Germany: Springer, 2010, pp. 1–14.
[27] S. Paris and F. Durand, "A fast approximation of the bilateral filter using a signal processing approach," in *Proc. Eur. Conf. Comput. Vis.* Berlin, Germany: Springer, 2006, pp. 568–580.
[28] F. Porikli, "Constant time O(1) bilateral filtering," in *Proc. IEEE Conf. Comput. Vis. Pattern Recognit.*, Jun. 2008, pp. 1–8.
[29] Q. Yang, K.-H. Tan, and N. Ahuja, "Real-time O(1) bilateral filtering," in *Proc. IEEE Conf. Comput. Vis. Pattern Recognit.*, Jun. 2009, pp. 557–564.
[30] A. Adams, N. Gelfand, J. Dolson, and M. Levoy, "Gaussian KD-trees for fast high-dimensional filtering," in *Proc. ACM SIGGRAPH Papers*, 2009, pp. 1–12.
[31] K. He and J. Sun, "Fast guided filter," 2015, *arXiv:1505.00996*. [Online]. Available: http://arxiv.org/abs/1505.00996
[32] R. Gordon, R. Bender, and G. T. Herman, "Algebraic reconstruction techniques (ART) for three-dimensional electron microscopy and X-ray photography," *J. Theor. Biol.*, vol. 29, no. 3, pp. 471–481, Dec. 1970.
[33] P. Gilbert, "Iterative methods for the three-dimensional reconstruction of an object from projections," *J. Theor. Biol.*, vol. 36, no. 1, pp. 105–117, Jul. 1972.
[34] A. H. Andersen and A. C. Kak, "Simultaneous algebraic reconstruction technique (SART): A superior implementation of the ART algorithm," *Ultrason. Imag.*, vol. 6, no. 1, pp. 81–94, Jan. 1984.
[35] V. Vaish and A. Adams, "The (new) stanford light field archive," Comput. Graph. Lab., Stanford Univ., Stanford, CA, USA, Tech. Rep. 7, 2008, vol. 6, no. 7. [Online]. Available: http://lightfield.stanford.edu
[36] Z. Wang, A. C. Bovik, H. R. Sheikh, and E. P. Simoncelli, "Image quality assessment: From error visibility to structural similarity," *IEEE Trans. Image Process.*, vol. 13, no. 4, pp. 600–612, Apr. 2004.
[37] A. Mittal, A. K. Moorthy, and A. C. Bovik, "Referenceless image spatial quality evaluation engine," in *Proc. 45th Asilomar Conf. Signals, Syst. Comput.*, vol. 38, 2011, pp. 53–54.
[38] A. Mittal, A. K. Moorthy, and A. C. Bovik, "No-reference image quality assessment in the spatial domain," *IEEE Trans. Image Process.*, vol. 21, no. 12, pp. 4695–4708, Dec. 2012.
[39] D. G. Dansereau, O. Pizarro, and S. B. Williams, "Decoding, calibration and rectification for lenselet-based plenoptic cameras," in *Proc. IEEE Conf. Comput. Vis. Pattern Recognit.*, Jun. 2013, pp. 1027–1034.
[40] D. G. Dansereau, O. Pizarro, and S. B. Williams, "Linear volumetric focus for light field cameras," *ACM Trans. Graph.*, vol. 34, no. 2, pp. 1–15, 2015.

SHAN GAO received the B.S. degree in information and computing science from the Ningbo University of Technology, Ningbo, Zhejiang, China, in 2015, and the M.S. degree in applied mathematics from the Beijing Information Science and Technology University, in 2018. She is currently pursuing the Ph.D. degree in computational mathematics with Beijing Jiaotong University, Beijing, China. Her research interests include image reconstruction and computational imaging.

GANGRONG QU received the B.S. degree in mathematics from Jilin University, Jilin, China, in 1983. He is currently a Professor with the School of Science, Beijing Jiaotong University. His research interests are image reconstruction and compressed sensing. He is also interested in light field reconstruction.